Visual Neuroscience (2003), **20**, 335–348. Printed in the USA.

DOI: 10.1017/S0952523803203126

Functional relationship between nucleus isthmi and tectum in teleosts: Synchrony but no topography

DAVID P.M. NORTHMORE AND SHAWN P. GALLAGHER
Department of Psychology, University of Delaware, Newark

(RECEIVED March 12, 2002; ACCEPTED June 9, 2003)

Abstract

Neural activity in the optic tectum was compared with activity in the nucleus isthmi (NI) of both goldfish and sunfish with the aim of understanding how the two brain structures interact to process visual information. The two species yielded very similar results. Superficial tectum responds reliably to visual stimulation with topographically organized receptive fields; deep tectum and NI respond to stimulation throughout the field of the contralateral eye and habituate rapidly. Bursts of large-amplitude spiking in NI occur spontaneously and in response to contralateral visual stimulation. These NI bursts correlate with activity bursts across the tectal lobe on the same side, especially in the deeper layers. NI bursts may also synchronize with spiking activity in deep tectum. Trains of small-amplitude spikes in NI can be elicited by both ipsilateral and contralateral stimulation, but are not reflected in tectal activity. Simultaneous recordings from two sites in one NI were almost identical, suggesting that NI operates as a functional unit, broadcasting the same message across the ipsilateral tectal lobe.

Keywords: Optic tectum, Nucleus isthmi, Goldfish, Sunfish, Fish vision, Synchrony

Introduction

Electrical recordings from the optic tectum of fishes have established that each retina projects an orderly map onto the surface of the opposite tectal lobe (Schwassmann & Kruger, 1965). When a microelectrode tip is inserted into the superficial layers, spiking activity can be recorded in response to visual stimulation of the contralateral eye. This activity is strongest in the *stratum opticum* (SO) and *stratum fibrosum et griseum superficiale* (SFGS), the principal terminal layers of retinal fibers (Sharma, 1972; Meek, 1983; Schmidt et al., 1988; Kageyama & Meyer, 1988), and is reliably evoked by visual stimulation within localized receptive fields with precise retinotopic organization (Northmore, 1989). The mapping of the retinotectal projection using this activity has been the basis of many studies of the formation of ordered neural connections. Fish have played an important role in these studies because their optic fibers regenerate readily after damage and restore the retinotectal map (review: Sharma, 1993). Experience shows that the best mapping results are to be had by not penetrating too deeply with the microelectrode because, below the superficial layers of tectum, neural activity is unreliably evoked by visual stimulation, bursts spontaneously, and worst of all is not clearly retinotopic. One aim of this study was to make sense of the activity below SFGS by examining its relationship to the activity of nucleus isthmi (NI), a tegmental nucleus with reciprocal connections with the tectum (Luiten, 1981; Dunn-Meynell & Sharma, 1984; King & Schmidt, 1993; reviews: Gruberg, 1983; Wang, 1988). A correlation in activity between the two structures might be expected at the junction of SFGS and the layer beneath, the stratum griseum centrale (SGC), because it is there that the axons of the tectoisthmic projection originate and the isthmotectal projection terminates most densely (Meek, 1983; Xue et al., 2001).

The anatomical projections between the NI and optic tectum in fishes (Grover & Sharma, 1981; Sakamoto et al., 1981) (see Fig. 1), as in other vertebrates (Sereno & Ulinski, 1987; Güntürkün & Remy, 1990), are organized topographically. Most studies in fishes have described isthmotectal projections that are only ipsilateral; however, a few have found evidence that NI also projects contralaterally to the rostral tectum serving the binocular visual field (Dunn-Meynell & Sharma, 1984, Sas & Maler, 1986; Brandis & Saidel, 2001). Both ipsilateral and contralateral NI projections to tectum have been well documented in frogs where NI forms an intertectal relay necessary for the binocularity of tectal neurons (Gruberg & Lettvin, 1980; Grobstein & Comer, 1983). Electrophysiological studies of NI in various species have shown it to be visually responsive with receptive fields that reflect the topographic nature of its connections with tectum (Hunt et al., 1977; Sherk, 1979; Gruberg & Lettvin, 1980). In the case of fishes, only the perciform NI has been mapped electrophysiologically (Northmore et al., 1990; Northmore, 1991) and, surprisingly, it showed no evidence of visuotopography, being excited by visual stimuli throughout the field of the contralateral eye. One explanation is that the cells of NI are functionally coupled. The evidence, at least from perciforms, is that groups of NI cells exhibit dye coupling

Address correspondence and reprints to: David P.M. Northmore, Department of Psychology, University of Delaware, Newark, DE 19716, USA. E-mail: northmor@udel.edu

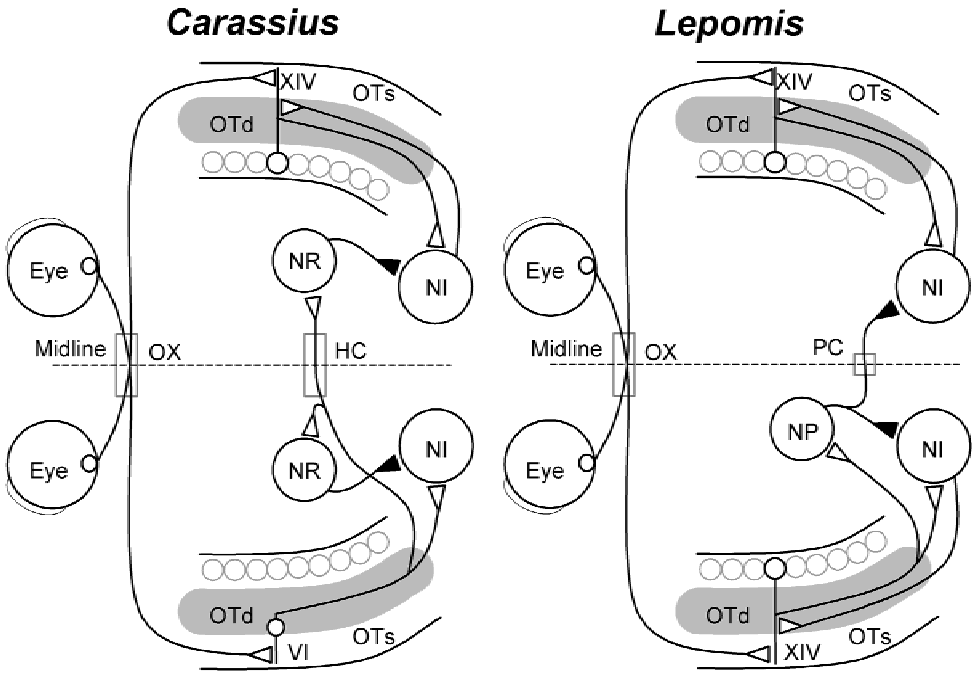

Fig. 1. Schematic of tectum-NI connections. Principal nuclei and connections of *Carassius* and *Lepomis* discussed in the text. For more detail see Xue et al. (2001), Striedter & Northcutt (1989), King & Schmidt (1993). Open triangles indicate presumed excitatory synapses, filled triangles presumed inhibitory synapses (Ito et al., 1982; King & Schmidt, 1993). Tectal cells (VI and XIV, Meek & Schellart, 1978) of *Carassius* and NP of *Lepomis* are depicted only unilaterally for clarity. HC: horizontal commissure; NI: nucleus isthmi; NP: nucleus pretectalis; NR: nucleus ruber; the lateral thalamic nucleus (Braford & Northcutt, 1983; King & Schmidt, 1993); OTd: deep optic tectum; OTs: superficial optic tectum; OX: optic chiasm; PC: posterior commissure; XIV: type XIV pyriform cell; and VI: type VI bipolar cell.

(Williams et al. 1983), indicating low-resistance interconnections, possibly formed by gap junctions seen in an ultrastructural study (Ito et al., 1982). To test the coupling idea, we have recorded with dual electrodes in NI.

These experiments were done on bluegill sunfish (*Lepomis macrochirus*), the perciform species used in an earlier study (Northmore, 1991), and on the goldfish (*Carassius auratus*), whose NI has been the subject of anatomical and physiological studies, but none that looked at visual responses. Comparison of the two species is interesting because the sources of input to NI in cyprinids differ from those in perciforms as shown in Fig. 1 (Striedter & Northcutt, 1989; King & Schmidt, 1993; Xue et al., 2001). The present experiments show that the neural activity in deep tectum is more closely related to activity in NI than it is to the activity in SFGS, immediately above, and that NI spatially integrates signals from tectum and broadcasts back to tectum.

Methods

Preparations and neural recording

Bluegill sunfish (*Lepomis macrochirus*, 8–15 cm standard length) and goldfish (*Carassius auratus*, 8–13 cm standard length) were obtained from a local hatchery (Hiram Peoples Hatcheries, New Providence, PA), kept in the laboratory at 20–24°C on a 14-h light/10-h dark cycle, and fed dried goldfish pellets. All procedures were identical for both species unless otherwise indicated and were approved by the University of Delaware Institutional Animal Care and Use Committee.

Before electrophysiological recording, fish were anesthetized by immersion in a solution of MS222 (Sigma Chemical, St. Louis, MO) buffered to neutral pH. Fish were then wrapped in wet paper towels and placed upright in a V-block holder provided with a metal mouth tube that supplied a continuous stream of aerated water during recordings and served as a connection to electrical ground. The midbrain was exposed by removing the overlying cranium and perimeningeal tissue and the wound margins were treated with a local anesthetic (Lidocaine gel, 2%). The head was stabilized with two stainless-steel struts that were clamped to each side of the V-block and extended to the lateral edges of the cranial opening. Fish were immobilized by cutting the spinal cord, which did not prevent saccadic eye movements. The eyes were prevented from moving in mapping experiments by applying Vetbond adhesive cement (3M, Minneapolis, MN) at the rostral or caudal pole of the orbit. The myopia of the eye in air was corrected with specially constructed contact lenses applied to the cornea (Northmore, 1989). We do not believe fish suffered serious discomfort after the MS222 anesthetic had worn off because before spinalization they did not struggle in the holder, and even after spinalization continued to make periodic eye and gill movements seen in intact, restrained animals.

Neural activity was recorded extracellularly with stainless-steel microelectrodes (FHC, Bowdoinham, ME) with tip resistances of 0.2–1 MΩ, and amplified with a bandpass of 0.3–3 kHz. In some experiments, the amplified signals were digitized at 12 kHz and stored in computer files for the analysis of spike waveforms. In other experiments, they were fed to leaky integrators that full-wave rectified and integrated the signals with a time constant of 15 ms; these signals were digitized at 200 Hz.

To record from tectum, a microelectrode was lowered onto the lateral surface of the left lobe at a rostrocaudal level halfway between the cerebellum and telencephalon. For recording superficial activity, the electrode was advanced to a depth of 100–200 μm. A hand-held, 1-cm square black flag was used to explore the multiunit visual responses and determine the center of their receptive fields. Multiunit receptive fields for this recording position on the tectal surface were approximately in the center of the field of view of the contralateral eye. For recording deep tectal activity, the electrode was advanced to 200–250 μm from the surface.

To record from NI, a microelectrode was positioned above the tectal surface 1.0–1.3 mm lateral to the midline at the rostrocaudal level of the anterior margin of the cerebellar corpus for *Lepomis*, and slightly caudal to the anterior margin of the cerebellar corpus for *Carassius*. Visually evoked multiunit responses were obtained at a depth of approximately 1500–1800 μm for both species. Dual electrode recordings in NI were made with stereotrodes, a pair of tungsten microelectrodes of 5–10 μm tip diameter and 0.5–1.0 MΩ resistance separated by 80–120 μm (WPI, Sarasota, FL). Individually, these electrodes were able to record isolated single units in tectum and in the oculomotor nucleus.

Electrode tip positions were marked by electrolytic lesions made with positive current of up to 5 μA for 10 s. At the conclusion of experiments, fish were overdosed with a 1:5000 solution of MS222 and the brains were removed and immediately frozen in isopentane at -30°C and then stored at -20°C for histology.

Visual stimuli

A stimulus array was made by gluing seven red light-emitting diodes (LEDs) (640 nm, 3.5×10^4 quanta$\cdot s^{-1} \cdot cm^{-2} \cdot sr^{-1}$, 200 ms, 3-deg angular subtense) to the back of a 15 $\times$ 20 cm screen of translucent white Plexiglas. The screen was set up normal to the visual axis of the fish's right eye. Five of the LEDs spaced at 25 deg formed a horizontal row; two others were placed 25 deg above and below the center LED, which was positioned in the receptive field of the electrode in superficial optic tectum (OTs). The screen was illuminated diffusely from above with tungsten light to provide a background radiance of 30 $\mu W/cm^2/sr$. For receptive-field mapping experiments, the LEDs were flashed for 100 ms in random order at 60-s intervals. Response habituation was tested by flashing the center LED three consecutive times before flashing one of the four neighboring LEDs.

Data analysis

The latencies and amplitudes of multiunit responses were measured from output records of the integrators described above. Mean response latencies were measured as the time between the stimulus onset and the time at which the integrator output reached 50% of peak amplitude. Response amplitudes were quantified by determining a mean baseline amplitude for the 100-ms period before each stimulus and subtracting it from the mean amplitude for the 100-ms period beginning at stimulus onset. Responses to different stimuli were compared by computing mean amplitudes as percentages of the largest response recorded at a given electrode site. In the figures these are referred to as "Relative Response%". Mean latencies and amplitudes were derived from 50 trials (10 $\times$ 5 fish), unless otherwise noted. *t*-tests were used for comparing two means and analysis of variance for comparing three or more means ($\alpha = 0.05$).

Results

Because the results from *Carassius* and *Lepomis* were similar, the descriptions apply to both, unless otherwise noted.

Extracellular activity recorded from nucleus isthmi

A metal microelectrode descending toward NI recorded bursts of spikes that were predominantly positive in polarity attaining peak amplitudes of 400 μV in *Carassius* and 1.0 mV in *Lepomis*. A further descent resulted in a reversal in the predominant polarity of the spike potentials, the reversal being more clearly seen in *Lepomis* than in *Carassius*. Lesion marking at this point placed the electrode tip in the shell of cell bodies covering the dorsomedial aspect of NI. Bursts of high-amplitude spikes occurred both spontaneously and in response to visual stimulation throughout the field of the contralateral eye. LED flashes and especially object movement were effective stimuli, but their effectiveness rapidly waned with repetition. NI spikes were variable in amplitude and waveform, making it impossible to isolate single units with consistent waveforms (see Fig. 11 upper, for a sample of spontaneous spiking activity). Fig. 2 shows histograms of spike amplitudes recorded from NI in *Carassius* evoked by LED stimuli, resembling previously published data from *Lepomis* (Northmore, 1991). Amplitudes are shown negative because the electrode tip was within the core where this is the predominant polarity of spikes. The continuous range of spike amplitudes is shown by the monotonic fall off in the histogram. Because of the variable NI waveforms, spike firing frequencies can only be given for percentiles of amplitudes. The largest spikes (>50% of maximum amplitude) occur in short bursts of typically four spikes at frequencies of up to 50/s.

LED flashes in the field of the ipsilateral eye also evoked spiking activity in NI, but of a different character from that evoked by contralateral field stimulation. Firstly, individual spike peak waveforms evoked by ipsilateral LEDs were only about 25% of the amplitude of the spikes evoked by contralateral LEDs. This can be seen in the amplitude histogram of Fig. 2 for *Carassius*. Secondly, ipsilateral stimulation generated relatively prolonged discharges of low-amplitude spiking that were distinct from the high-amplitude bursts evoked by contralateral stimulation. These differences in response characteristics can be seen in Fig. 3 showing typical records of integrated activity in *Carassius* in response to ipsilateral and contralateral stimulation.

Recordings within the core of NI sometimes yielded well-isolated spike potentials that were not obscured by the bursting of the large-spike discharges. These single units fired in trains, accelerating up to 40/s after LED stimulation, and could be driven by ipsilateral as well as contralateral visual stimulation. They may, therefore, be responsible for the low amplitude spiking mentioned above.

Responses of tectum and NI to contralateral visual stimulation

The spiking activity encountered in superficial optic tectum (OTs) consisted of multiunit bursts that occurred reliably to stimulation in the field of the contralateral eye, either with the hand-held flag or LED flashes. Marking the electrode tip position by lesions showed this activity to originate in SFGS, the primary target

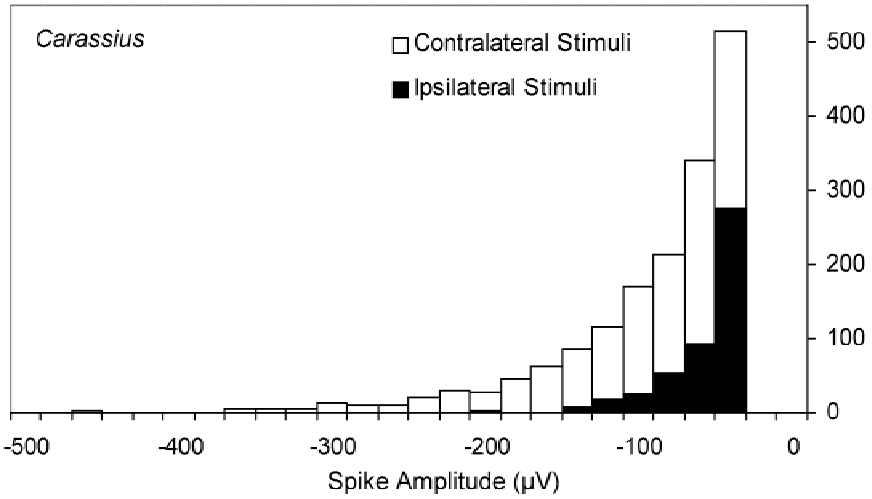

Fig. 2. Histograms of spike amplitudes recorded in nucleus isthmi of *Carassius* evoked by ipsilateral and contralateral eye stimuli. Stimuli were 100-ms LED flashes centered in the fields of the contralateral or ipsilateral eyes. Spikes were counted during the 100-ms stimulus and recorded from the core of the nucleus where spikes were mainly negative-going. Results of 20 ipsilateral and 20 contralateral stimulus presentations from two fish.

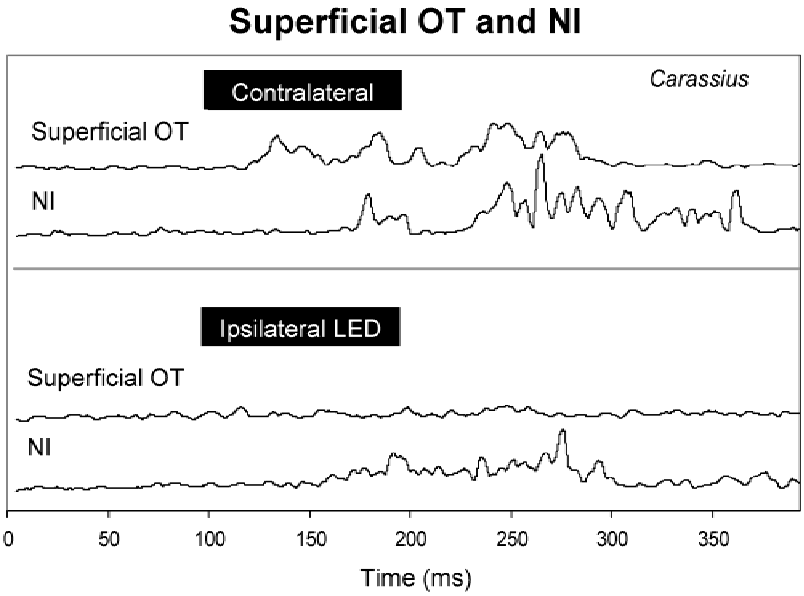

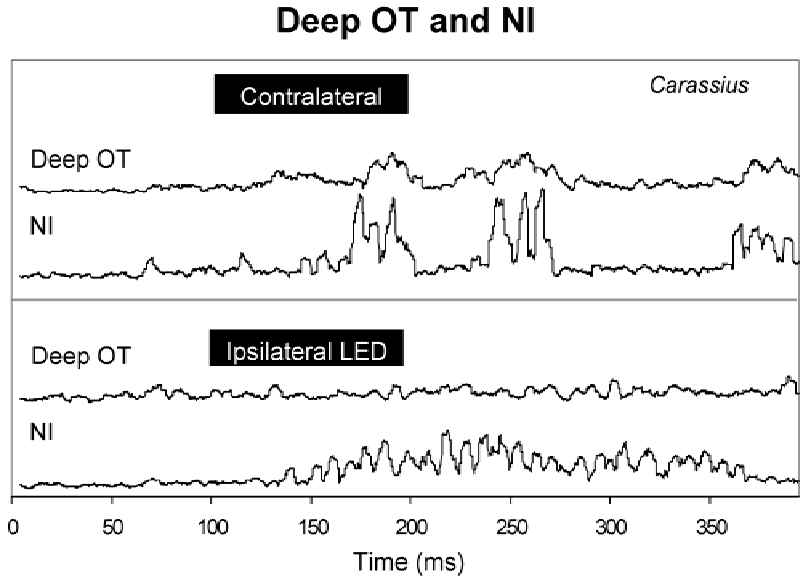

Fig. 3. Samples of integrated activity during stimulation with 100-ms LED flashes in the ipsilateral and contralateral fields of *Carassius*. (Top) Simultaneous records from superficial OT and NI. (Bottom) Simultaneous records from deep OT and NI.

lamina for retinal ganglion cells. This activity exhibited well-defined, roughly circular receptive fields. The open bar graphs of Fig. 4 shows averaged integrated activity recorded from OTs to LED flashes separated by 25 deg in the visual field in one specimen of *Carassius*. LED flashes at greater eccentricities evoked multiunit bursts whose magnitude declined with distance from the receptive-field center. The extreme temporal and nasal LEDs generated very little response. Recordings were made from more rostral and caudal positions in OTs to confirm that all the LEDs in the array were within the eye's visual field. Very similar results were obtained for *Lepomis*.

Repeatedly flashing a LED in the center of the electrode's multiunit receptive field evoked responses from OTs without habituation. This is shown for *Lepomis* in Fig. 5 (open bars) where averaged multiunit amplitudes are plotted for three consecutive 100-ms flashes of the center LED, presented at 60-s intervals. No response was less than 75% of the maximum response and mean responses were similar for each of the three flashes ($P > 0.3$).

As the electrode tip advanced through OTs to the deeper layers of optic tectum we call OTd, the activity changed character, bursting spontaneously and responding more weakly and erratically to visual stimuli. Lesions at this depth were found at the junction of SFGS and SGC, or within SGC. Amplitudes of average LED-evoked responses are compared with those in OTs in Fig. 6. LEDs flashed anywhere on the array were equally effective in OTd (Fig. 4, gray bars) with latencies that were significantly greater than OTs (Fig. 7). Repeated LED flashes at a single location in the visual field resulted in response habituation. Fig. 5 (gray bars) shows significantly smaller average response amplitudes on the second and third flashes at the same field position. When the fourth flash was presented at a new position, 25 deg away from the first, the response amplitude recovered partially (Fig. 5 "Switch") showing that habituation was visuotopically specific. Fig. 5 shows results with *Lepomis*, but very similar data were obtained with *Carassius*.

The visual response properties of NI differed markedly from those of OTs (Fig. 3), but had much in common with those of OTd. As Fig. 4 shows, there was no evidence of visuotopography in the responses of NI; bursts of high-amplitude spiking could be evoked equally by any of the seven LEDs in the array ($P < 0.01$). Analysis of integrated activity records, such as those of Fig. 3, showed no relationship between NI response latency and LED position ($P > 0.5$). NI responded to LED flashes at latencies that were significantly longer than those of OTs ($P < 0.05$) (Fig. 7). Pronounced habituation occurred to LED flashes at a single location (Fig. 5, black bars); the second in a series of three flashes often evoked no significant activity and the mean response amplitudes associated with the second and third flashes were less than 25% of the amplitude of the first response. When the fourth flash was presented at 25 deg away from the first, the response amplitude was comparable to that of the first response (Fig. 5 "Switch"), showing that habituation was visuotopically specific.

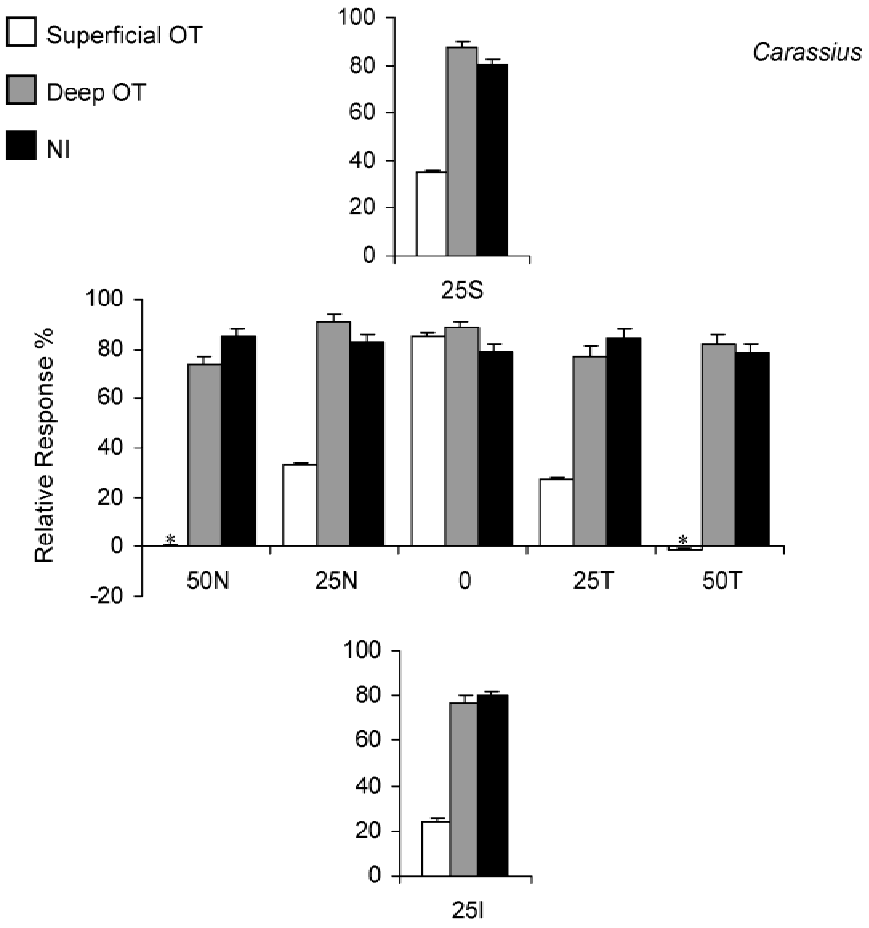

Fig. 4. Amplitude of integrated activity recorded from superficial tectum, deep tectum, and nucleus isthmi of *Carassius* in response to 100-ms LED flashes in different parts of the contralateral visual field. Ten responses were recorded from each of seven stimulus positions in five fish. Labels indicate LED positions in degrees relative to the center of the LED array (N: nasal, T: temporal, S: superior, and I: inferior). Mean responses recorded from superficial OT varied as a function of LED position ($P < 0.01$), whereas those recorded from deep OT and NI did not. Mean responses recorded from deep OT and NI were greater than 0 for all tested LED positions. Mean responses recorded from superficial OT were only significant for stimuli within 25 deg of the visual axis. $*$ = no response ($P < 0.01$).

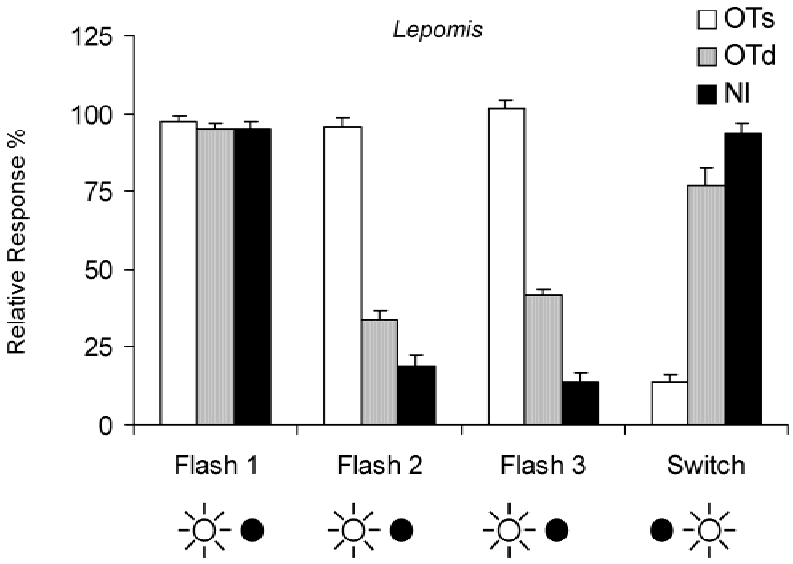

Fig. 5. Visual response habituation. Mean response amplitudes (+SEM) recorded from OTs, OTd, and NI of *Lepomis* in response to four consecutive 100-ms LED flashes presented at 60-s intervals. Flashes 1–3 were in the center of the OTs multiunit receptive field; the fourth flash (Switch) was 25 degrees from the original location. Mean responses recorded from OTd and NI varied as a function of flash sequence ($P < 0.01$), whereas those recorded from OTs did not. OTd and NI habituated to repeated stimulation at the same location, but recovered when the location was changed. The mean NI response to the fourth flash did not differ significantly from the mean response to the first flash ($P > 0.5$). Each bar is the average of ten responses from three individual *Lepomis*. Very similar results were obtained with *Carassius*.

Correlations between NI and tectal activity

To investigate the relationship between tectum and NI, simultaneous recordings were made in both structures on the same side of the brain. Fig. 8 shows samples of integrated activity recorded simultaneously over 40 s from NI and OTs, and from NI and OTd of *Lepomis*. Bursts of high-amplitude spikes, both visually evoked and spontaneous, occurred in NI together with bursts of activity in OTs and in OTd, but the NI–OTd correlations were always higher than the NI–OTs correlations (compare *r* in Fig. 8). Correlation coefficients were also calculated between pairs of recordings such as those shown in Fig. 3 using integrated data during and after LED stimulation. The results averaged from five individuals of each species are shown in Fig. 9. When LEDs were flashed in the contralateral field, the correlation between OTd and NI was significantly greater than that between NI and OTs ($P < 0.05$) for both species. When LEDs were flashed in the field ipsilateral to NI, the small-spike activity in NI was not related to activity in tectum on the same side, resulting in near-zero average correlations for both species.

The correlations between NI and OTd activity on a shorter time scale were explored in five specimens of *Lepomis* using unintegrated electrical recordings. The two uppermost traces in Fig. 10A show sample activity waveforms from the core of NI, where the spikes are predominantly negative going, together with simultaneously recorded waveforms from OTd. Shown below is the running correlation coefficient calculated from the two records over a moving 5-ms window. During the first 250 ms, there were some six synchronous bursts in both structures leading to large negativity in the running correlations. At about 300 ms, there was an NI burst without an accompanying OTd burst. Not shown in this figure are instances, which were common, of OTd bursts that occurred without NI bursts. Strongly negative correlation, indicating periods of synchrony, occurred in bouts lasting 10–200 ms. Close synchrony of spiking in the two structures is demonstrated in Fig. 10 (B–D). In the cross correlograms (Fig. 10B), computed from the spike records in Fig. 10A, a sharp negative peak ($r = -0.47$) appeared at 0-ms offset, indicating a high degree of synchrony. Cross-correlating nonsimultaneous NI and OTd records as a control showed no such peaks (Fig. 10C). Fig. 10D shows five pairs of simultaneously recorded spikes occurring in the core of NI and OTd, again showing precise synchrony between spike waveforms. When the electrode was raised out of the core, the NI spike potentials became mainly positive in polarity and all the correlation coefficients became positive.

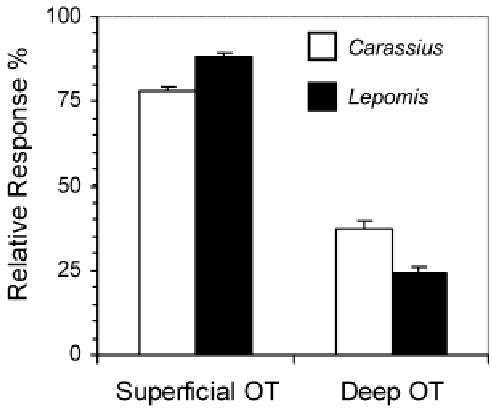

Fig. 6. Comparison of stimulus-evoked response amplitudes in superficial and deep optic tectum. Mean amplitudes of integrated multiunit bursts (+SEM) recorded in response to a 100-ms LED flash in the center of the tectal receptive field. Mean responses recorded from superficial OT were greater than those recorded from deep OT for each species ($P < 0.01$). Each mean was calculated from 50 responses (10 × 5 animals).

NI potentials elicited by electrical stimulation of tectum

Given the synchrony of spiking in NI and OTd, it was of interest to measure the conduction time between the two structures. In *Lepomis*, field potentials were recorded from the shell of NI in response to electrical stimulation of the ipsilateral tectal surface at the same position that most tectal recordings were made. The waves evoked by supramaximal stimulation resembled those described by Williams et al. (1983) and examples are shown in Fig. 11. The first wave occurred with latencies between 1.8 and 2.4 ms (mean = 2.15 ms, two fish) and followed stimulus shocks

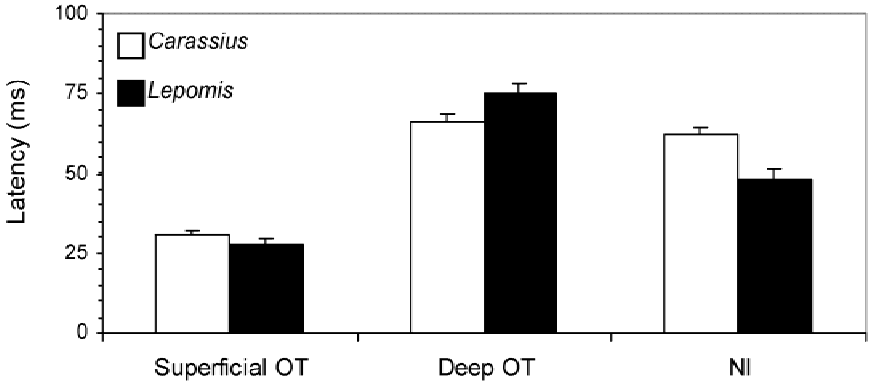

Fig. 7. Average response latencies (+SEM) of integrated activity recorded from superficial OT, deep OT, and NI in response to a 100-ms LED flash in the visual field of the contralateral eye. Latencies for each location varied significantly within species with the exception of deep OT and NI of *Carassius* ($P > 0.05$). Each mean was calculated from 50 responses (10×5 animals).

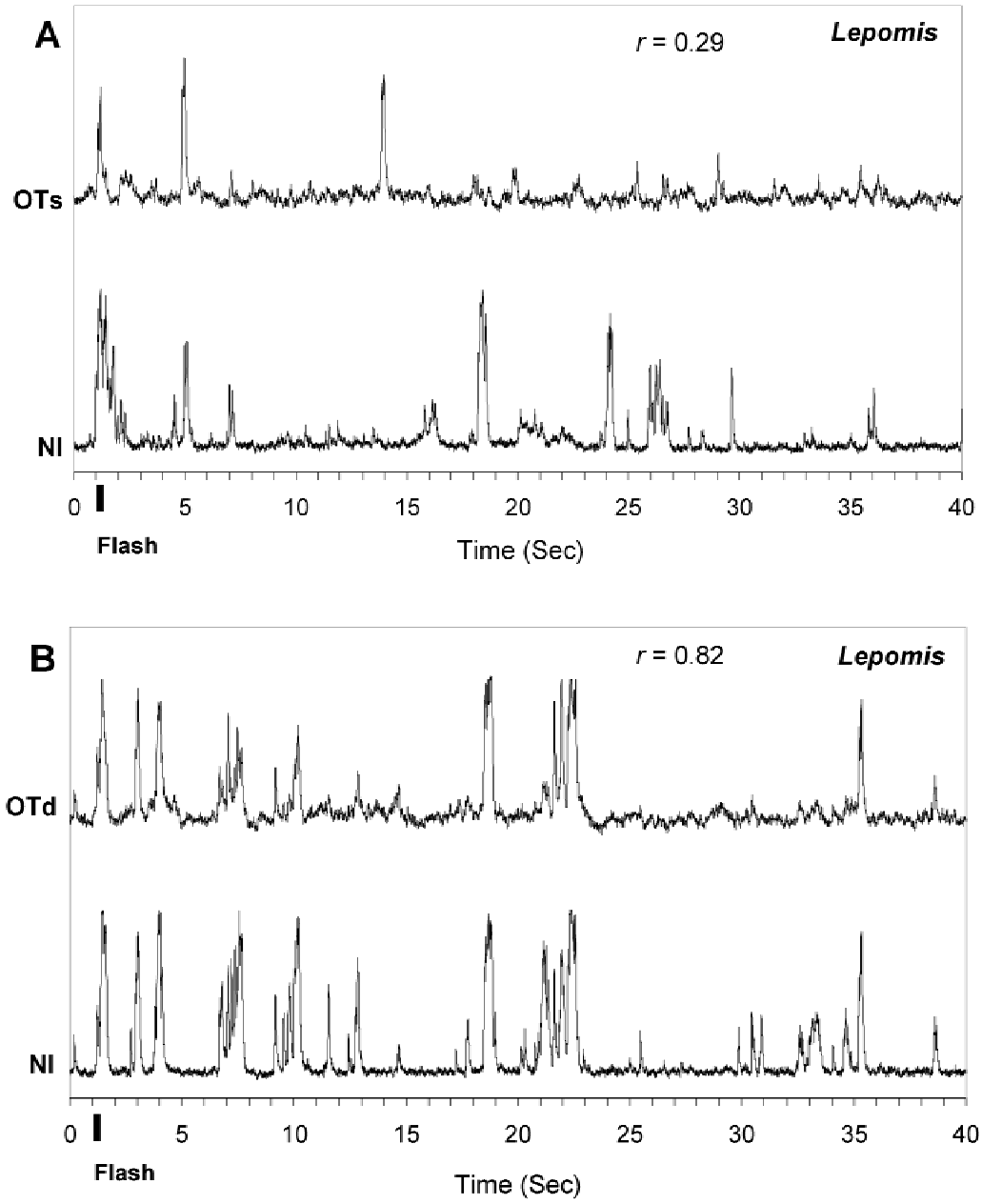

Fig. 8. Integrated activity recorded simultaneously in *Lepomis*—(A) from superficial OT (OTs) and NI, and (B) from deep OT (OTd) and NI. A single 200-ms LED flash was presented at T= 1.0 s. Correlation coefficients calculated over the entire 40 s given by *r*.

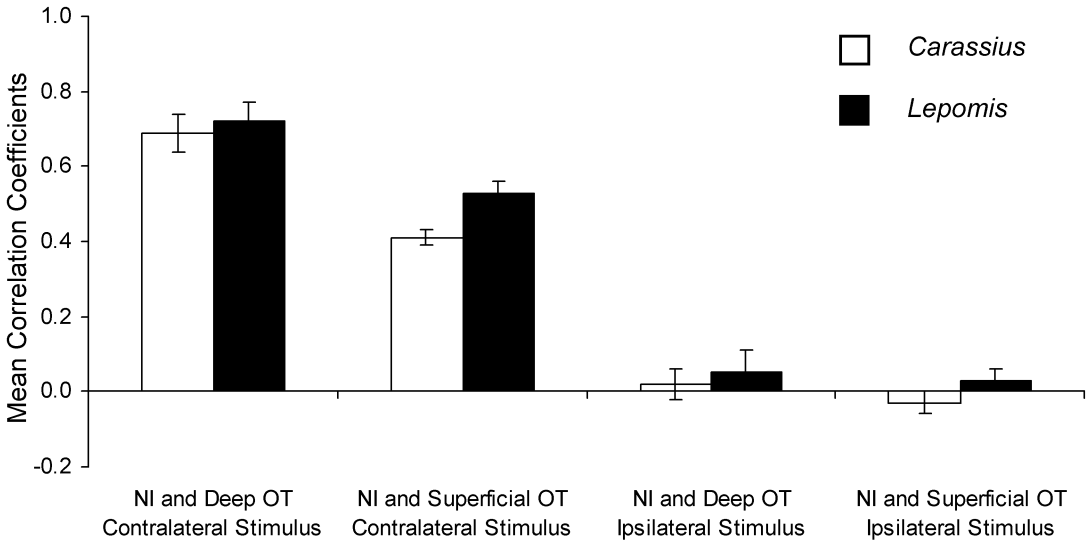

Fig. 9. Correlations between activity in OT and NI evoked by contralateral and ipsilateral stimulation. Correlation coefficients were calculated from pairs of records similar to those in Fig. 2, using 300 ms of data starting at LED onset. Each bar shows mean correlation coefficients of ten record pairs from five fish of both species. The LED stimulus was presented to the contralateral or the ipsilateral eye.

at frequencies of over 100 Hz. Each tectal shock also elicited three or four additional waves, starting at about 4-ms latency, which failed to follow high stimulation rates. Williams et al. (1983) interpreted the first wave as the antidromic spike response of isthmotectal cells, and the subsequent waves as orthrodromically driven spikes of NI cells. Fig. 11 (top) shows a record in which typical spontaneous spiking occurred before the electrical stimulus to the tectum was delivered. These spontaneous spikes exhibited a range of amplitudes that, while smaller than the antidromic spike, encompassed the amplitudes of the orthrodromic spikes.

Stereotrode recordings

The possibility that NI cells are coupled was investigated by using stereotrodes with 80–100 μm tip separations in order to compare activity from two positions separated rostrocaudally in the NI shell. Diameters of NI cell bodies in both *Carassius* and *Lepomis* are less than 10 μm so that a stereotrode positioned in the densely packed shell of the nucleus recorded from two locations separated by approximately eight to ten cell bodies.

When both electrodes of the stereotrode pair were positioned within the shell of NI, the spike waveforms from the two electrodes were strikingly similar (Fig. 12). Correlating the two records during the 200-ms LED flash gave significant ($P < 0.001$) correlation coefficients ranging from 0.45 to 0.87 (mean 0.71; SD 0.12) in *Carassius*, and from 0.67 to 0.96 (mean 0.85; SD 0.08) in *Lepomis*. As a control for correlation due to noise and neural responses time locked to stimulation, correlations were calculated between recordings taken on different stimulus trials. These shuffled correlations were always close to zero. Figs. 13A and 13B are cross-correlograms calculated from recordings taken with the paired electrodes from individuals of both species showing typical interelectrode phase differences of less than 0.2 ms. Correlations between the two electrodes were negative when one electrode tip sampled positive-going spikes from outside the shell and the other sampled negative-going spikes from within the core, which argues against an artifactual correlation due to cross-talk between channels.

As an additional comparison, the same stereotrode pair was used to record stimulus-evoked activity from two sites in OTs. Significant interchannel correlations were again observed ($P < 0.001$), but significantly smaller than those from NI ($P < 0.001$), showing that similarity of waveforms between the stereotrodes was not always obtained.

Discussion

Electrical activity of NI

The electrical activity of NI in teleosts is unusual. NI generates high-amplitude spike potentials with variable waveforms that are, nevertheless, very similar from moment to moment at different locations across the nucleus. The change in polarity of the spike potentials from positive to negative as the electrode penetrates the nucleus indicates that current sinks are located in the core, presumably activated by the excitatory tectoisthmic synapses on NI cell dendrites that ramify there (Ito et al., 1982). Whether the spike potentials are excitatory postsynaptic potentials (EPSPs) or regenerative action potentials cannot be settled for certain by the present extracellular recordings, but the latter interpretation is supported by the experiments in which NI was excited by electrical stimulation of tectum. As Fig. 11 shows, the NI spikes that Williams et al. (1983) interpreted as driven transynaptically by tectal shocks were comparable in amplitude and width to spikes that occurred spontaneously or those evoked by visual stimulation.

Our recordings of very similar electrical waveforms at widely separated positions in the nucleus (Figs. 12 & 13) suggest that cells of NI are coupled, causing a number of them to discharge in unison. An anatomical basis for coupling is the finding of Ito et al. (1982) in the percomorph, *Navodon modestus*, that tectoisthmic terminals form conventional synapses as well as "close membrane appositions" with dendrites in the core of NI. The latter contacts could provide low-resistance bridges between NI cells. This would account for the observations of Williams et al. (1983) in *Perca fluviatilis* that Lucifer Yellow injected into one cell diffuses into a

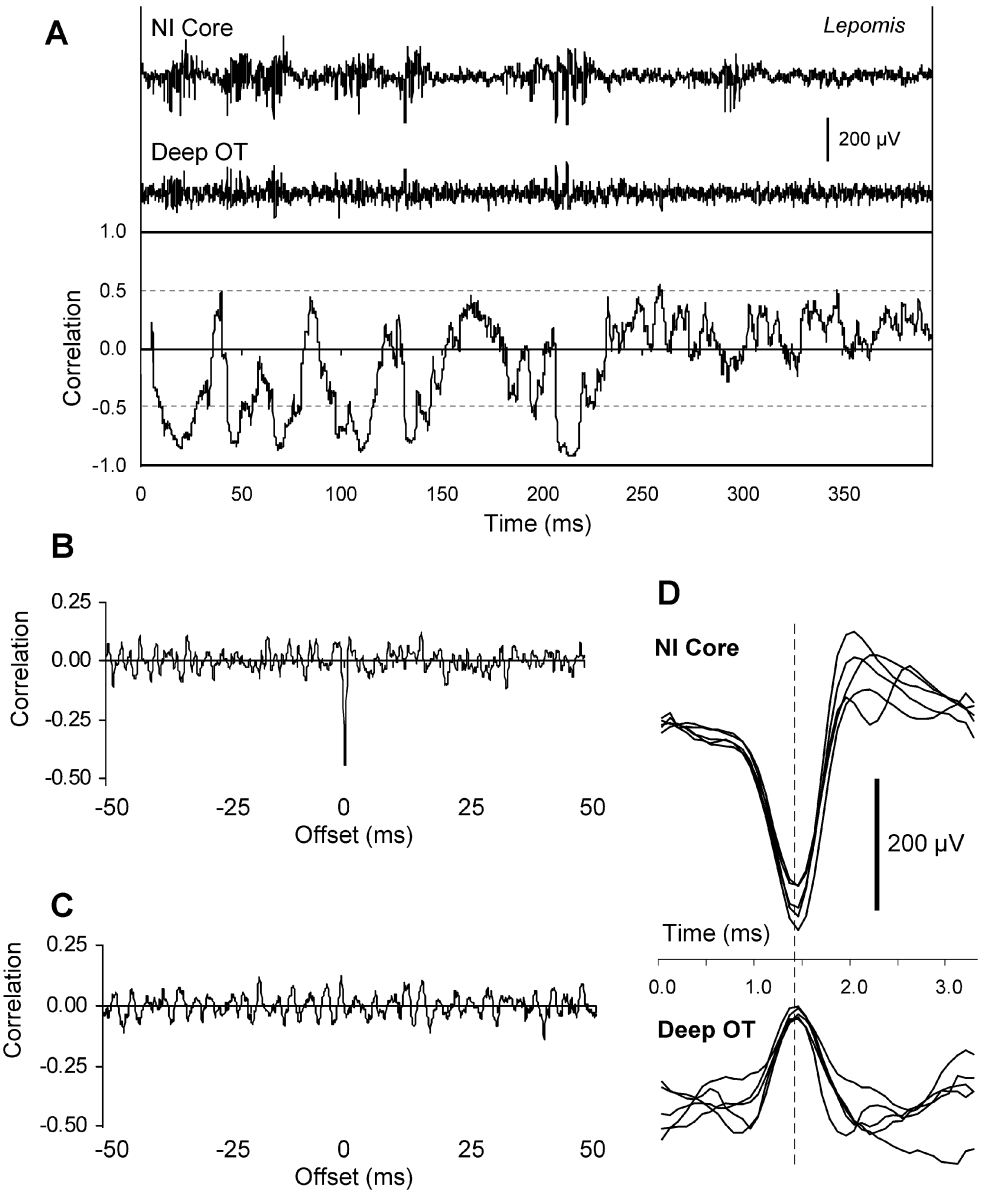

Fig. 10. Synchronization of spikes in nucleus isthmi core and deep optic tectum. (A) Spontaneous activity from the core of nucleus isthmi (NI) and deep optic tectum (OT) of *Lepomis*, with a continuous plot of the correlation between the records (5-ms window). (B) Cross-correlogram of the records in A. (C) Control correlogram calculated from two nonsimultaneous records. (D) Superimposed records of five negative potentials recorded from the core of NI and five coincident positive potentials recorded from deep OT. Waveforms sampled at 12 kHz.

number of neighboring cells in NI, and that the extracellular spike potentials closely resemble the waveforms recorded intracellularly from NI cells. The variable amplitude and waveform of the spikes recorded extracellularly from NI is probably due to varying numbers of cells firing together.

Visually evoked activity of NI

Although anatomical studies in teleosts have described a topographic projection from tectum to NI (Sakamoto et al., 1981), and from NI to tectum (Grover & Sharma, 1981; Dunn-Meynell & Sharma, 1984), visually driven NI activity exhibited no clear receptive-field organization in either *Carassius* or *Lepomis*. NI responded uniformly to visual stimuli presented over wide regions of the contralateral visual field with bursts of high-amplitude spikes (Figs. 3 & 4). Northmore (1991) had previously shown in *Lepomis* NI with more detailed LED mapping that the high-amplitude spikes were evoked by stimuli throughout the field of the contralateral eye, with no evidence of visuotopography in either the amount of firing or in its temporal patterning. The possibility of coupling between cells of NI leading to synchronous firing could explain this lack of visuotopography. An alternative explanation with uncoupled NI cells is that tectoisthmic afferents possess very large visual receptive fields and/or a high degree of convergence onto NI cells. However, even given perfect synchrony of tectoisthmic afferents, it seems improbable that NI

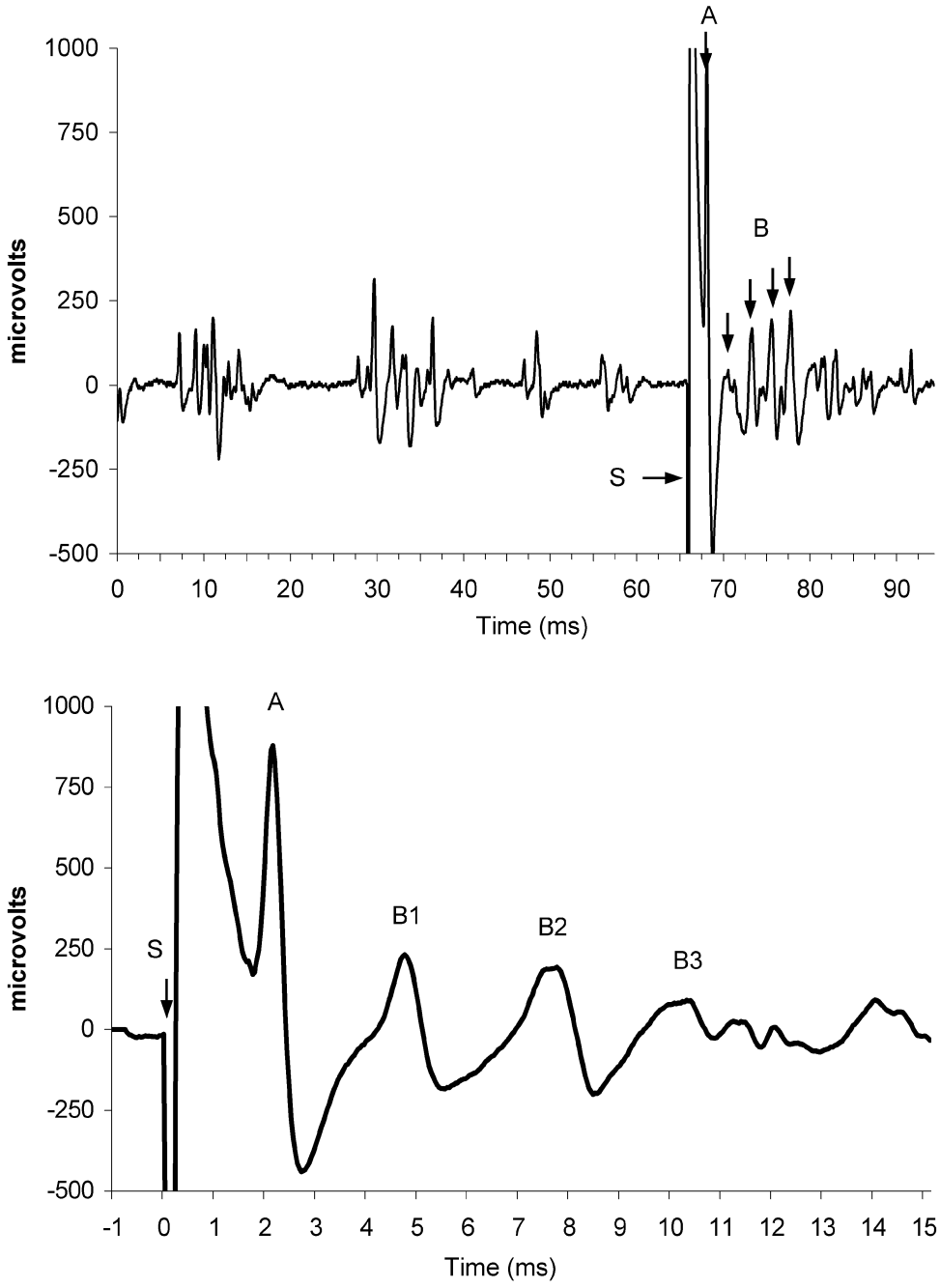

Fig. 11. Top: Extracellular potentials recorded from the shell of NI in *Lepomis*. The record initially shows spontaneous bursting activity followed at 65 ms by a single 10-μs electric shock(s) to tectum. This evoked a large, short latency antidromic spike (A) and four orthodromically driven potentials (B). Bottom: Average of five NI responses evoked by shocks to tectum showing antidromic (A) and orthodromic potentials (B1–B3) as described by Williams et al. (1983).

cells would be capable of synchronizing their firing across the 100 μm spanned by the stereotrodes, and with the consistency we observed.

The responses of NI rapidly habituate when a stimulus is presented repeatedly at one location in the visual field, but recover when the stimulus moves to a different location (Fig. 5). Habituation, therefore, is retinotopically specific and probably occurs in tectal cells or, possibly, at tectoisthmic synapses. Previous electrophysiological investigations have described habituating tectal units (Jacobson & Gaze, 1964; O'Benar, 1976; Schellart & Spekreijse, 1976). Activity in OTd also habituated (Fig. 5), but it is impossible to tell whether this represents the habituation of tectal cells or of the NI input to OTd.

Functional relationships between NI and OT

The response properties of OTs in fishes are well known, and our data showing OTs' activity to be locked to visual stimulation, both

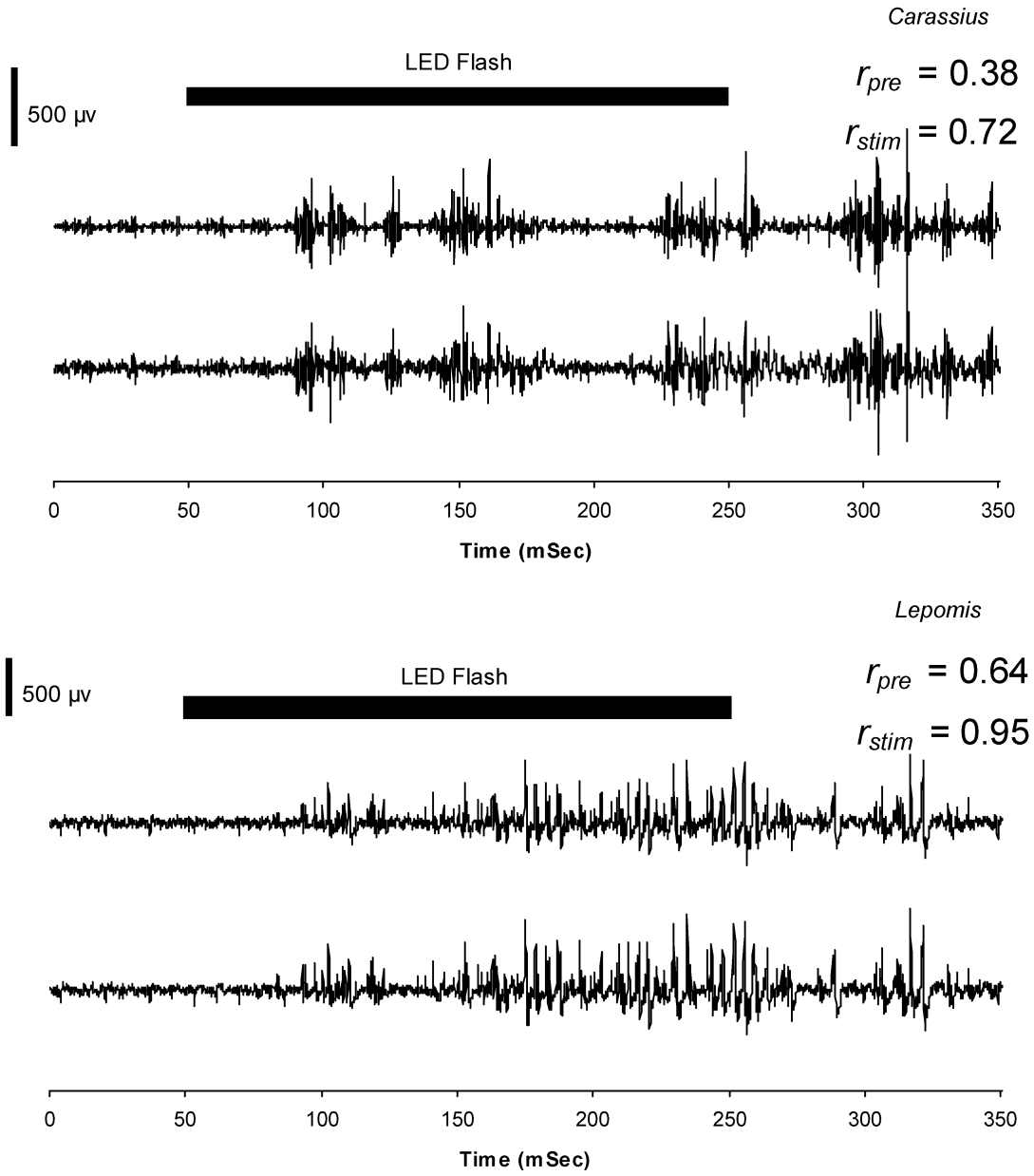

Fig. 12. Stereotrode records from nucleus isthmi. Two stereotrode recordings taken from the nucleus isthmi neuropil shell of *Carassius* (top) and *Lepomis* (bottom). The solid bar above each pair of records represents a 200-ms LED flash occurring in the visual field contralateral to the nucleus. The records illustrate the nearly identical traces recorded from two locations separated by approximately 100 μm in the shell of nucleus isthmi. Correlation coefficients for the 50 ms preceding the LED flash (r_{pre}) and for the 200-ms stimulus period (r_{stim}) are displayed for each pair of records.

spatially and temporally is not new; much less considered is the activity just beneath, in OTd, which is not so obviously related to visual stimulation. (See Figs. 3–9, which contrast the properties of OTs and OTd.). The superficial activity reflects retinal properties, presumably because it is generated close to retinal terminals. The deeper activity is consonant with the reported properties of isolated tectal units, of which relatively few have been recorded intracellularly and identified as known cell types (O'Benar, 1976; Schellart & Spekreijse, 1976; Niida et al., 1980; Guthrie & Sharma, 1991). These units tend to have visual receptive fields that are large, complex in spatial arrangement, habituating, and generally difficult to characterize. How the transformation occurs is unknown, but the present results showing correlations between activity in OTd and NI suggest that NI plays a role.

Measures of visuotopography (Fig. 4), stimulus-evoked response habituation (Fig. 5), amplitude (Fig. 6), and latency (Fig. 7) in NI and tectum, and the correlations between them (Figs. 8–10) suggest a closer functional relationship between NI and OTd than between NI and OTs. This can be understood by reference to the anatomy of the tectoisthmic cell types and the layers of termination of afferents to tectum originating in the retina and in NI.

The principal layers of termination of retinal ganglion cells in tectum are in OTs, specifically the SO and SFGS. The most numerous tectal cell type, the pyriform or Type XIV of Meek and

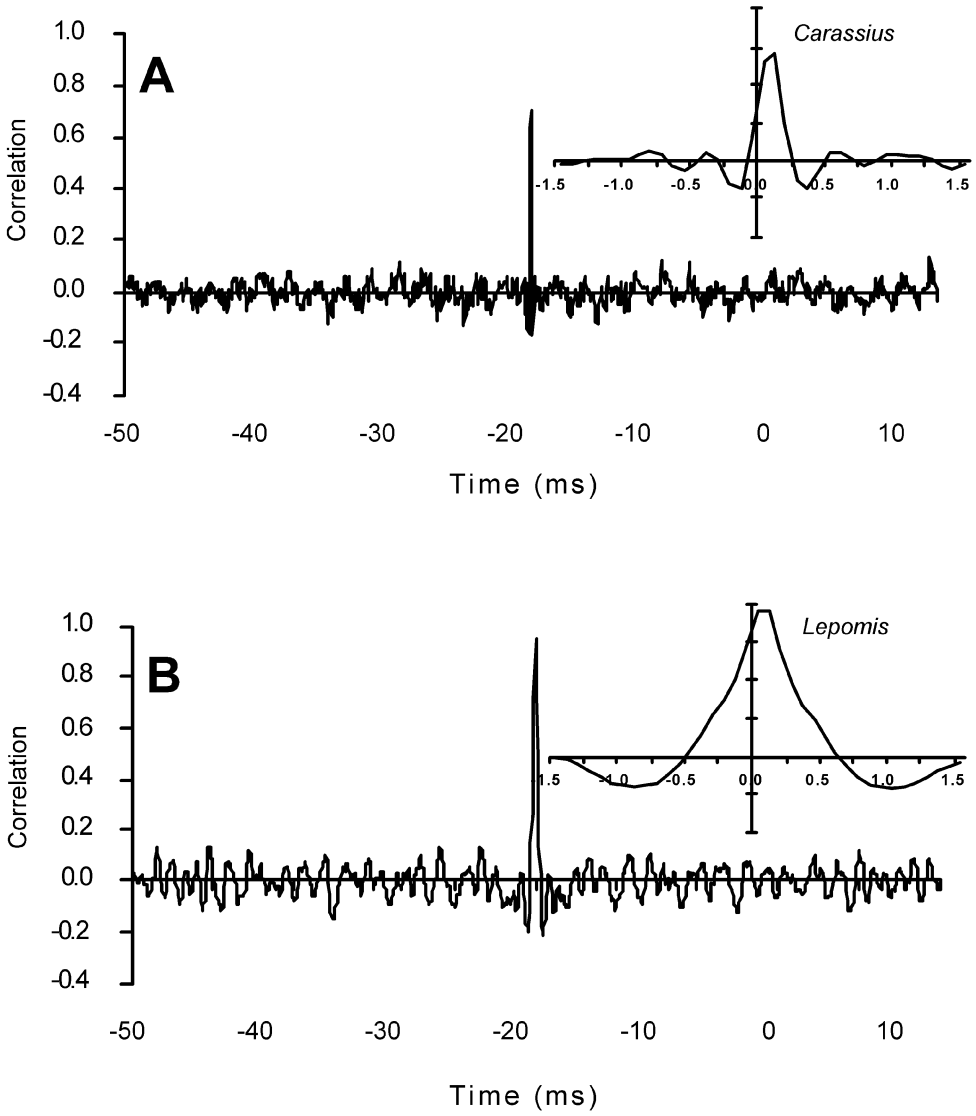

Fig. 13. Cross-correlations of recordings made with a stereotrode pair in the shell of NI in *Carassius* (A) and *Lepomis* (B). The insets illustrate high-resolution views of each cross-correlogram.

Schellart (1978), receives synaptic input in these layers (Meek, 1983) and could therefore be driven by visual stimulation. The visually evoked activity in OTs has often been attributed to retinal terminals because receptive fields recorded there are topographically arranged and resemble retinal ganglion cell receptive fields (Jacobson & Gaze, 1964; Cronly-Dillon, 1964). However, experiments blocking synapses in tectum pharmacologically suggests that OTs activity in goldfish is partly, if not mostly, postsynaptic in origin (Gallagher & Northmore, 1997; Stirling et al., 2001; Kolls & Meyer, 2002), and therefore reflects spike generation in the dendrites of retinorecipient cells like the Type XIV. A dendritic origin has also been proposed for visually evoked spiking activity in superficial frog tectum (Grant & Lettvin, 1991).

A subset of Type XIV cells projects to NI in both *Carassius* (King & Schmidt, 1993) & *Lepomis* (Striedter & Northcutt, 1989). In cyprinid fishes, but not in perciforms, another tectal cell type, the fusiform Type VI of Meek and Schellart (1978), also projects to NI (King & Schmidt, 1993; Xue et al., 2001) (See Fig. 1). Tectoisthmic axons originate just above the boundary of SFGS and SGC (Meek & Schellart, 1978; Ito et al., 1981; Xue et al., 2001) close to the depth we have called OTd.

The fibers efferent from NI project to the ipsilateral tectal lobe and have been described as branching in all the layers from SO to SGC, but most densely at the boundary between SFGS and SGC (Meek, 1981; Ito et al., 1982; Striedter & Northcutt, 1989; King & Schmidt, 1993). However, Xue et al. (2001), in a study of a cyprinid and a perciform using sensitive-tracing methods, describe NI efferents descending through SO and SFGS to terminate mostly in deep SGC. Thus, the anatomical distribution of isthmotectal terminals corresponds generally to our results that show stronger correlations between activity in NI and OTd, than between NI and OTs (Figs. 8–10). An electrode in OTd records activity that is strongly influenced by NI, perhaps directly from NI terminals or secondarily from tectal cell dendrites innervated by NI terminals. Driving of OTd by NI is also suggested by the longer latency of the OTd response to visual stimulation, at least in *Lepomis* (Fig. 7). However, OTd, as the boundary region of SFGS and SGC, also includes the axon initial segments of many tectal cell types,

including the Type VI and Type XIV tectoisthmic cells, so these too are likely sources of spiking activity that we may have recorded. What can be said is that those spikes recorded in OTd that are closely synchronized with NI spikes (Fig.10D) cannot be from NI terminals because of the 2–3 ms isthmotectal pathway delay.

Synchrony between tectum and NI

Dual electrode recordings in NI and tectum showed that bursting activity in NI is often, but not invariably, accompanied by bursting activity in OTd. This can be seen in sample records of integrated activity (Figs. 3 & 8) that provide a running average of all activity over some 15 ms. The combined data from several individuals of both species (Fig. 9) confirm a high degree of correlation between NI and OTd, and lesser but still significant correlation between NI and OTs.

Comparing the waveforms from NI and OTd on a finer time scale showed that the large spikes of NI, when synchronized with spikes in OTd, do so to within ± 0.25 ms (Fig. 10D). Cross-correlograms of the two waveforms (Fig. 10B) always peaked around 0 ms. The sign of the correlation depended on whether the NI spikes were recorded outside the shell (positive) or inside the core (negative), showing that the synchrony cannot be an artifact of cross-talk between the two recording channels.

The close synchrony between spikes in NI and tectum raises the question of the conduction delay between the two structures. The delay in the isthmotectal pathway, about 2 ms in *Lepomis* and 3 ms in *Carassius* (King & Schmidt, 1993), corresponds to a conduction velocity of about 0.5 m/s. This is too slow for axons to generate spikes at both sites within 0.25 ms or to account for cross-correlograms that peak at 0 ms. Instead, the synchrony is probably the result of phase locking between reciprocally connected isthmic and tectal neurons. These interconnections are excitatory (Williams et al. 1983; King & Schmidt 1993) and phase locking can occur, at least theoretically, between neurons with excitatory reciprocal connections despite substantial conduction delays between them (Gerstner et al., 1996).

The running correlations (Fig. 10A) indicated bouts of synchrony during bursts of large-spike activity in NI. However, not all NI bursts produced corresponding OTd activity. In these experiments synchrony was readily observed during spontaneous bursting in NI. Further experiments need to be done to see how synchrony is influenced by sensory stimulation because of the role it may play in feature binding and attention (Crick & Koch, 1990; Niebur et al., 2002)

NI responses to ipsilateral visual-field stimulation

Northmore (1991) reported that a class of small-spike potentials in *Lepomis* NI could be evoked by visual stimuli in either the ipsilateral or contralateral visual field. These small potentials were attributed to the terminals of what Xue et al., 2001 call the nucleus pretectalis (NP) (see Fig. 1). In *Lepomis* and other perciforms, NP receives monosynaptic input from ipsilateral tectum and projects thick myelinated fibers bilaterally to make synaptic contact with NI dendrites and somata (Ito et al., 1982; Striedter & Northcutt, 1989; Xue et al., 2001). Morphological criteria suggest that these synapses are inhibitory (Ito et al., 1982). Bilateral inhibitory projections from NP to NI explain a previous finding in *Lepomis* that a stimulus in the ipsilateral visual field inhibits the firing of NI to a stimulus in the contralateral visual field (Northmore, 1991).

In *Carassius* also, ipsilateral visual-field stimulation evokes small-spike activity in NI (Figs. 2 & 9), but the pathways mediating it in cyprinids appear to differ from those in perciforms. Cyprinid NI, instead of receiving input from NP, which appears to be lacking in cyprinids, receives thick myelinated fibers from a tegmental nucleus, nucleus ruber, and finer fibers from Type VI neurons in the SFGS of tectum (Braford & Northcutt, 1983; King & Schmidt, 1993; Xue et al., 2001). Although both of these inputs to NI are from ipsilateral sources, crossed connections to nucleus ruber (King & Schmidt, 1993; Xue et al., 2001) provide a path by which ipsilateral visual stimuli could inhibit NI in cyprinids.

Conclusion

In both *Carassius* and *Lepomis*, extracellular recordings from NI showed (1) large-spike bursts that occurred spontaneously and in response to stimuli presented throughout the field of the contralateral eye, (2) retinotopic habituation of responding with repeated stimulation, and (3) small-spike activity in response to stimuli throughout the field of the ipsilateral eye. Activity in NI was closely related to that in OTd, the source of tectoisthmic axons and the primary target of isthmotectal fibers, often synchronizing precisely with it. Electrical activity recorded simultaneously from different parts of NI were almost identical, suggesting that its cells are coupled, and that NI broadcasts the same message across the ipsilateral tectal lobe. The nontopographic character of this message and its response to salient, and especially threatening stimuli, as we show in a subsequent paper (Gallagher & Northmore, in preparation), suggest that it informs tectum of significant events allowing it to select stimuli and initiate behavioral responses accordingly.

References

Braford, M.R. & Northcutt, R.G. (1983). Organization of the diencephalon and pretectum of the ray-finned fishes. In *Fish Neurobiology*, ed. Davis, R.E. & Northcutt, R.G., pp. 117–163. Ann Arbor, Michigan: University of Michigan Press.

Brandis, A. & Saidel, W.M. (2001). Nucleus isthmi: The modulator of binocular vision in fish. *Bulletin of the New Jersey Academy of Sciences* **46**, 22.

Crick, F. & Koch, C. (1990). Some reflections on visual awareness. *Cold Spring Harbor Symposium on Quantitative Biology* **55**, 953–962.

Cronly-Dillon, J.R. (1964). Units sensitive to direction of movement in the optic tectum of the goldfish. *Nature* (London) **203**, 214–215.

Dunn-Meynell, A.A. & Sharma, S.C. (1984). Changes in the topographically organized connections between the nucleus isthmi and the optic tectum after partial tectal ablation in adult goldfish. *Journal of Comparative Neurology* **227**, 497–510.

Gallagher, S.P. & Northmore, D.P.M. (1997). The effect of cobalt blockade on stimulus-evoked activity in the goldfish optic tectum. *Investigative Ophthalmology and Visual Science* **38**, s361.

Gerstner, W., van Hemmen, J.L. & Cowan, J.D. (1996). What matters in neuronal locking? *Neural Computation* **8**, 1653–1676.

Grant, A.C. & Lettvin, J.Y. (1991). Sources of electrical transients in tectal neuropil of the frog *Rana pipiens*. *Brain Research* **192**, 313–325.

Grobstein, P. & Cromer, C. (1983). The nucleus isthmi as an intertectal relay for the ipsilateral oculotectal projection in the frog, *Rana pipiens*. *Journal of Comparative Neurology* **217**, 54–74.

Grover, B.G. & Sharma, S.C. (1981). Organization of extrinsic tectal connections in goldfish (*Carassius auratus*). *Journal of Comparative Neurology* **196**, 471–488.

Gruberg, E.R. (1983). Recent work on the nucleus isthmi and its niche in the visual system. In *Progress in Nonmammalian Brain Research*, Vol. I, ed. Nistico, G. & Bolis, L., pp. 159–174. Boca Raton, Florida: CRC Press.

Gruberg, E.R. & Lettvin, J.Y. (1980). Anatomy and physiology of a binocular system in the frog *Rana pipiens*. *Brain Research* **192**, 313–325.

Güntürkün, O. & Remy, M. (1990). The topographical projection of the nucleus isthmi pars parvocellularis (Ipc) onto the tectum opticum in pigeon. *Neuroscience Letters* **111**, 18–22.

Guthrie, D.M. & Sharma, S.C. (1991). Visual responses of morphologically identified tectal cells in the goldfish. *Vision Research* **31**, 507–524.

Hunt, S.P., Streit, P., Kunzle, H. & Cuenod, M. (1977). Characterization of the pigeon isthmo-tectal pathway by selective uptake and retrograde movement of radioactive compounds and by Golgi-like horseradish peroxidase labeling. *Brain Research* **129**, 197–212.

Ito, H., Tanaka, H., Sakamoto, N. & Morita, Y. (1981). Isthmic afferent neurons identified by the retrograde HRP method in a teleost, *Navodon modestus*. *Brain Research* **207**, 163–169.

Ito, H., Sakamoto, N. & Takatsuji, K. (1982). Cytoarchitecture, fiber connections, and ultrastructure of nucleus isthmi in a teleost (*Navodon modestus*) with a special reference to degenerating isthmic afferents from optic tectum and nucleus pretectalis. *Journal of Comparative Neurology* **205**, 299–311.

Jacobson, M. & Gaze, R.M. (1964). Types of visual responses from single units in optic tectum and optic nerve of the goldfish. *Quarterly Journal of Experimental Physiology* **49**, 199–204.

Kageyama, G.H. & Meyer, R.L. (1988). Laminar histochemical and cytochemical localization of cytochrome oxidase in the goldfish retina and optic tectum in response to deafferentation and during regeneration. *Journal of Comparative Neurology* **335**, 123–148.

King, W.M. & Schmidt, J.T. (1993). Nucleus isthmi in goldfish: *In vitro* recordings and fiber connections revealed by HRP injections. *Visual Neuroscience* **10**, 419–437.

Kolls, B.J. & Meyer, R.L. (2002). Spontaneous retinal activity is tonic and does not drive tectal activity during activity-dependent refinement in regeneration. *Journal of Neuroscience* **22**, 2626–2636.

Luiten, P.G.M. (1981). Afferent and efferent connections of the optic tectum in the carp (*Cyprinus carpio L.*). *Brain Research* **220**, 51–56.

Meek, J. (1981). A Golgi-electron microscope study of the goldfish optic tectum, I. Description of afferents, cell types and synapses. *Journal of Comparative Neurology* **199**, 149–173.

Meek, J. (1983). Functional anatomy of the tectum mesencephali of the goldfish. An explorative analysis of the functional implications of the laminar structural organization of the tectum. *Brain Research Reviews* **6**, 247–297.

Meek, J. & Schellart, N.A.M. (1978). A Golgi study of goldfish optic tectum. *Journal of Comparative Neurology* **182**, 89–122.

Niebur, E., Hsiao, S.S. & Johnson, K.O. (2002). Synchrony: A neuronal mechanism for attentional selection? *Current Opinion in Neurobiology* **12**, 190–194.

Niida, A., Oka, H. & Iwata, K.S. (1980). Visual responses of morphologically identified neurons in the crucian carp. *Brain Research* **201**, 361–371.

Northmore, D.P.M. (1989). Quantitative electrophysiological studies of regenerating visuotopic maps in goldfish—II. Delayed recovery of sensitivity to small light flashes. *Neuroscience* **32**, 749–757.

Northmore, D.P.M. (1991). Visual responses of nucleus isthmi in a teleost fish (*Lepomis macrochirus*). *Vision Research* **31**, 525–535.

Northmore, D.P.M., Guthrie, S.D. & Banks, J.R. (1990). Responses of the nucleus isthmi of perch recorded intracellularly and free-swimming. *Investigative Ophthalmology and Visual Science* **31**, s394.

O'Benar, J.D. (1976). Electrophysiology of neural units in goldfish optic tectum. *Brain Research Bulletin* **1**, 529–541.

Sakamoto, N., Ito, H. & Udea, S. (1981). Topographic projections between the nucleus isthmi and the optic tectum in a teleost, *Navodon modestus*. *Brain Research* **224**, 225–234.

Sas, E. & Maler, L. (1986). Identification of a nucleus isthmi in the weakly electric fish *Apteronotus leptorynchus* (Gymnotiformes). *Brain, Behavior, and Evolution* **28**, 170–185.

Schellart, N.A.M. & Spekreijse, H. (1976). Shapes of receptive field centers on optic tectum of goldfish. *Vision Research* **16**, 1018–1020.

Schmidt, J.T., Turcotte, J.C., Buzzard, M. & Tieman, D.G. (1988). Staining of regenerated optic arbors in goldfish tectum: Progressive changes in immature arbors and a comparison of mature regenerated arbors with normal arbors. *Journal of Comparative Neurology* **269**, 565–591.

Schwassmann H.O. & Kruger L. (1965). Organization of the visual projection upon the optic tectum of some freshwater fish. *Journal of Comparative Neurology* **124**, 113–126.

Sereno, M.I. & Ulinski, P.S. (1987). Caudal topographic nucleus isthmi and the rostral nontopographic nucleus isthmi in the turtle, *Pseudemys scripta*. *Journal of Comparative Neurology* **261**, 319–346.

Sharma, S.C. (1972). The retinal projections in the goldfish. An experimental study. *Brain Research* **39**, 213–223.

Sharma, S.C. (1993). Neural specificity revisited. In *Formation and Regeneration of Nerve Connections*, ed. Sharma, S.C. & Fawcett, J.W., pp. 248–257. Boston, Massachusetts: Birkhäuser.

Sherk, H. (1979). Connections and visual field mapping in the cat's tectoparabigeminal circuit. *Journal of Neurophysiology* **42**, 1656–1668.

Stirling, R.V., Bartlett, C.A., Dunlop, S.A. & Beazley, L.D. (2001). Light evoked responses recorded from the optic tectum are postsynaptic. *International Union of Physiological Sciences*. Abstract 1260.

Striedter, G.F. & Northcutt, R.G. (1989). Two distinct visual pathways through the superficial pretectum in a percomorph teleost. *Journal of Comparative Neurology* **283**, 342–354.

Wang, S.-R. (1988). The nucleus isthmi is a visual center: Neuroanatomy and electrophysiology. In *Vision: Structure and function*, ed. Yew, D.T., So, K.F. & Tsang, D.S.C., pp. 301–364. Teaneck, New Jersey.

Wang, S.-R., Yan, K., & Wang, Y.-T. (1981). Visual field topography in the frog's nucleus isthmi. *Neuroscience Letters* **23**, 37–41.

Williams, B., Hernandez, N. & Vanegas, H. (1983). Electrophysiological analysis of the teleostean nucleus isthmi and its relationship with the optic tectum. *Journal of Comparative Physiology A* **152**, 545–554.

Xue, H.-G., Yamamoto, N., Yoshimoto, M., Yang, C.-Y. & Ito, H. (2001). Fiber connections of the nucleus isthmi in the carp (*Cyprinis carpio*) and Tilapia (*Oreochromis niloticus*). *Brain, Behavior, and Evolution* **58**, 185–204.